Electronic Supplementary Information (ESI)

A graphene oxide scaffold-encapsulated microcapsule for polysulfides-rocked long life lithium-sulfur batteries

Xirong Lin,[‡,a] Chaoyu Yang,[‡,b] Tianli Han,[c] Jinjin Li,[*,a] Zhonghua Chen,[*,d] Haikuo Zhang,[a] Kai Mu,[b] Ting Si,[*,b] Jinyun Liu[*,c]

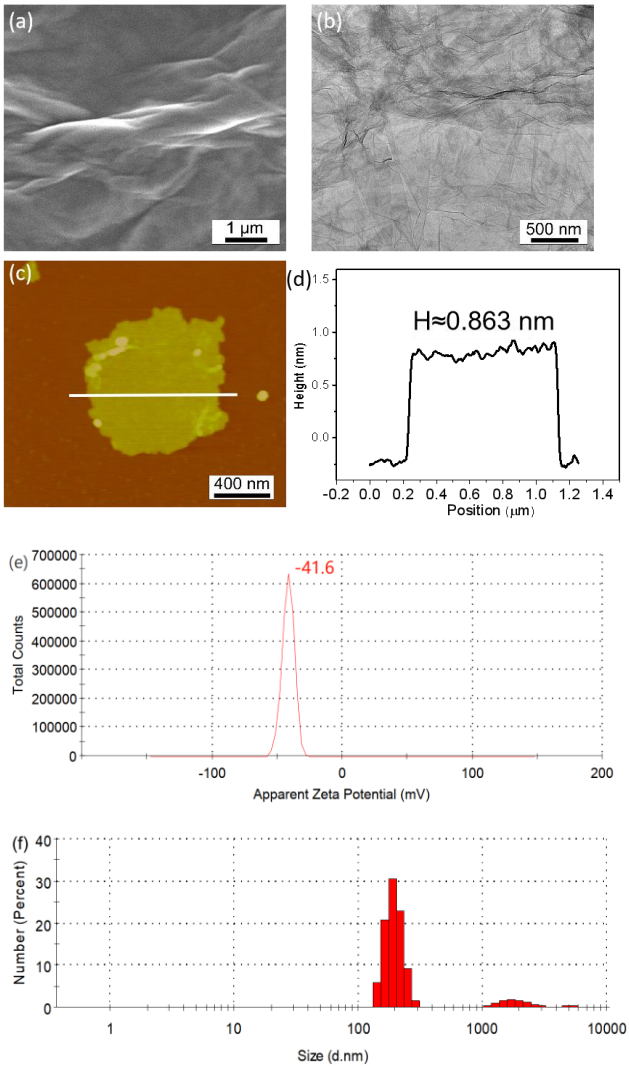

Fig. S1 (a) SEM, (b) TEM, (c) AFM images, (d) height profile, (e) Zeta potential and (f) size distribution of the GO nanosheets.

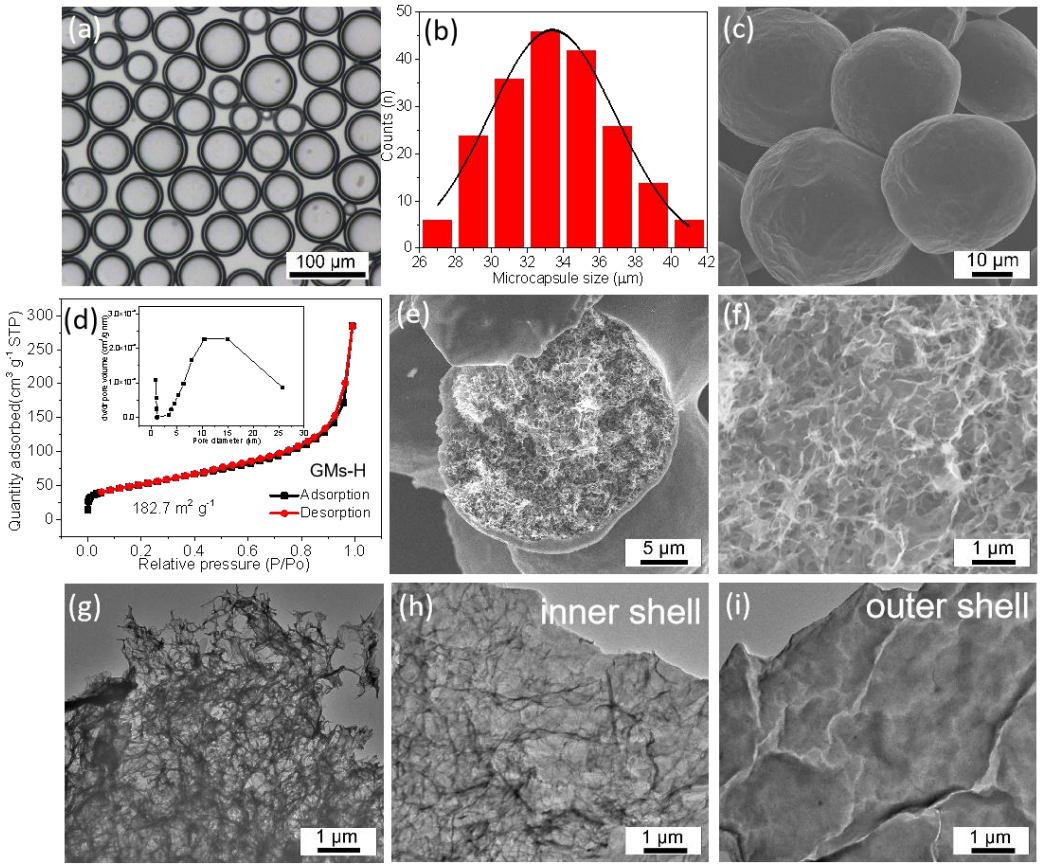

Fig. S2 Characterizations of the GMs-H. The (a) optical image and (b) corresponding size-distribution of the microcapsules after UV-curing. (c) SEM image and (d) Nitrogen adsorption/desorption isotherms of GMs-H. Inset in (d) shows the pore-size distribution. (e) Cross-section SEM image of GMs-H. (f) SEM and (g) TEM images of inner core. TEM images of (h) inner and (i) outer shell of the GMs-H.

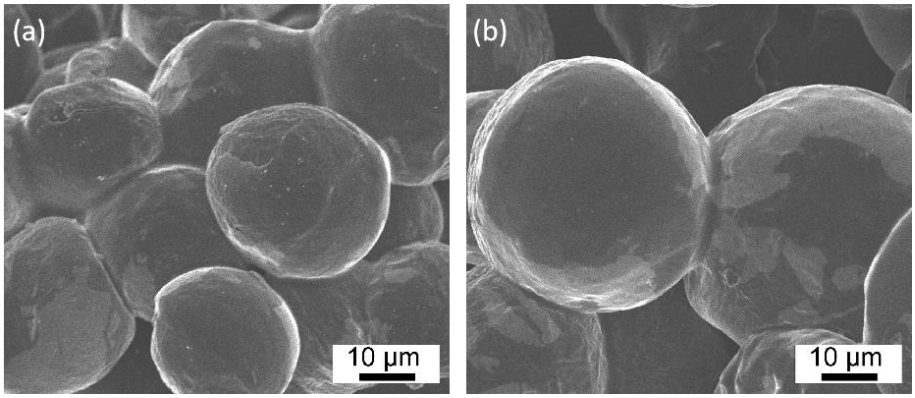

Fig. S3 (a,b) SEM images of the GSMs-H.

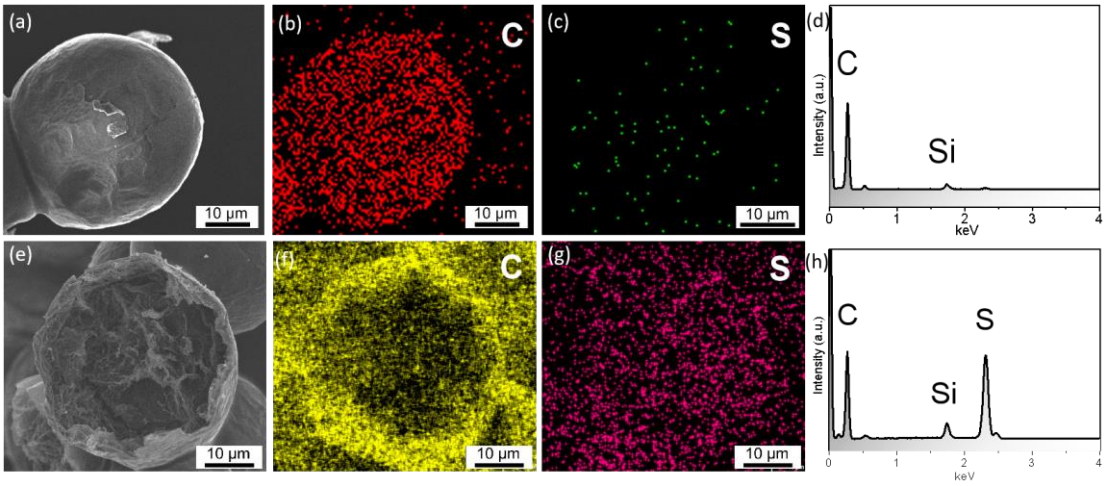

Fig. S4 (a) SEM image, (b,c) elemental mapping, and (d) EDS spectrum of a GSMs-H. Inset in (a) presents the corresponding line-scanning curves. (e) SEM, (f,g) elemental mapping images, and (h) EDS spectrum of a manually-broken GSMs-H.

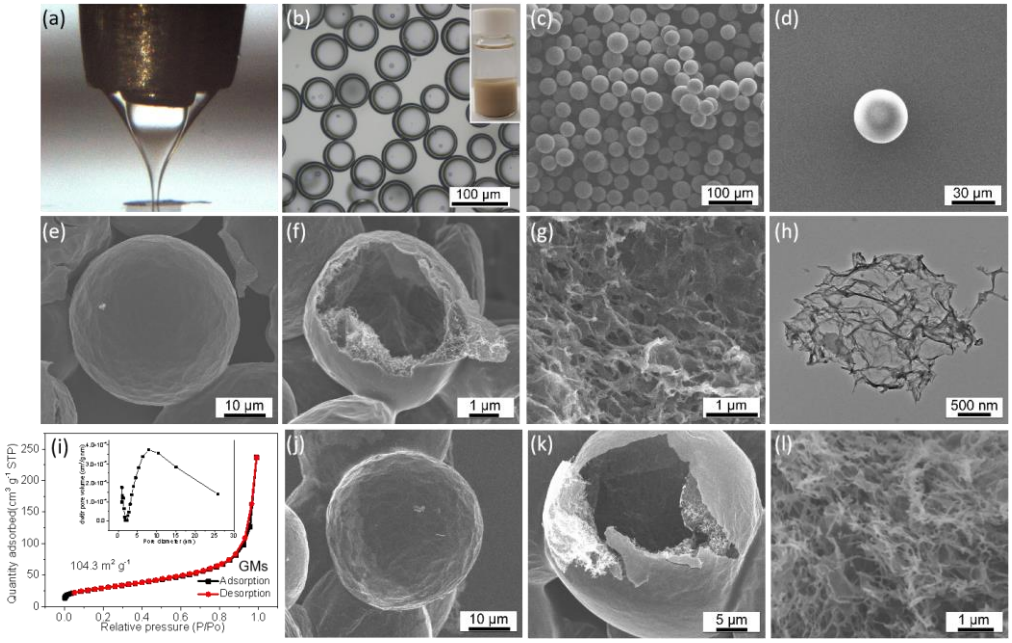

Fig. S5 (a) Optical images of a stable cone. (b) Optical and (c, d) SEM images of the GMs prepared by using a low concentration of GO solution (1 mg L^{-1}) after UV-curing. (e,f) SEM images of the GMs. (g) SEM and (h) TEM images of inner core for the GMs. (i) N_2 adsorption/desorption isotherms and pore-size distribution of the GMs. (j-l) SEM images of the GSMs and corresponding inner core after loading sulfur.

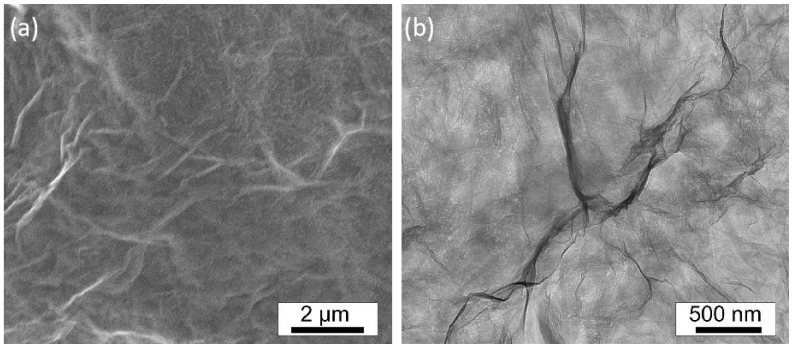

Fig. S6 (a) SEM and (b) TEM images of the GSSs.

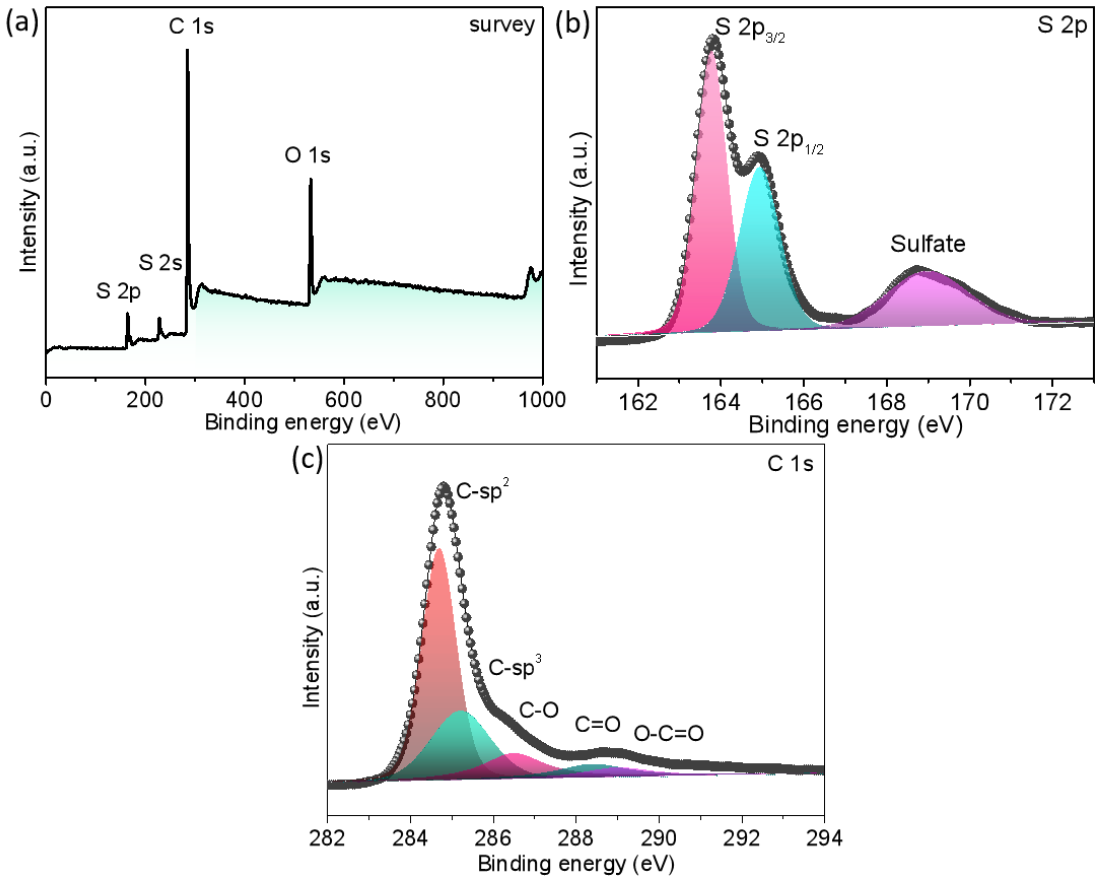

Fig. S7 XPS spectra of the GSMs-H: (a) survey spectrum, (b) S 2p, and (c) C 1s.

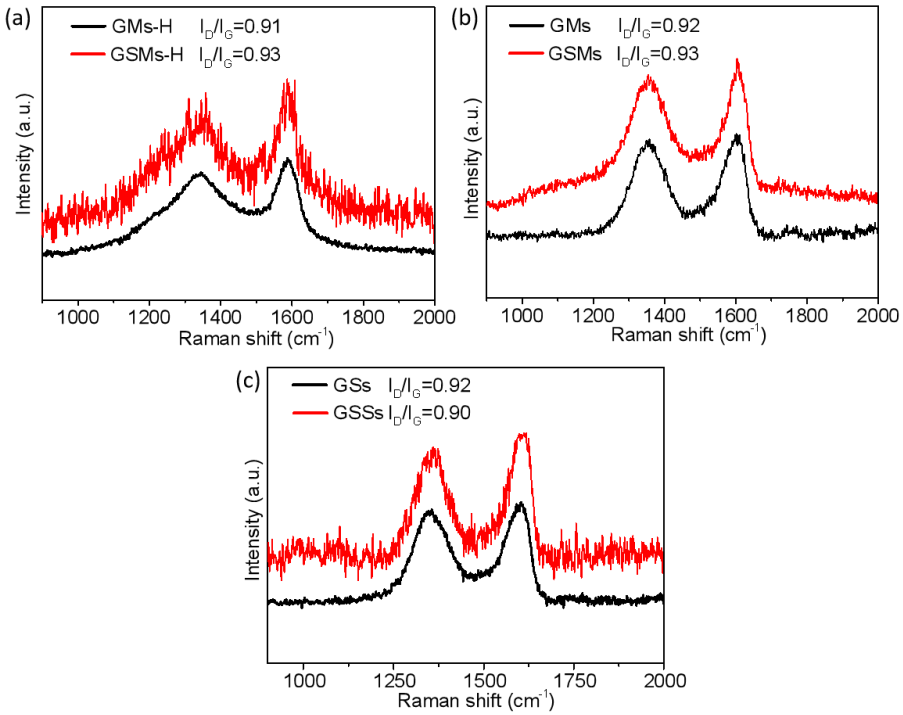

Fig. S8 Raman spectra of the (a) GMs-H and GSMs-H, (b) GMs and GSMs, (c) GSs and GSSs.

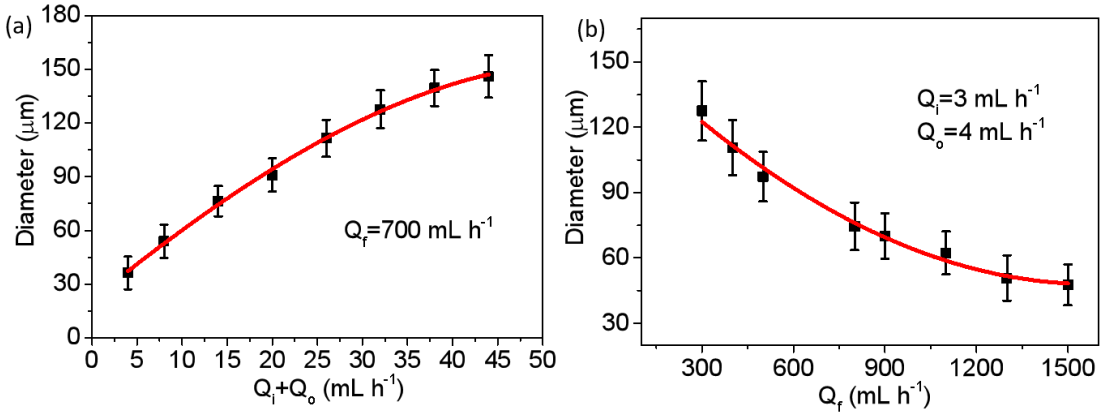

Fig. S9 The relationship between diameter of GMs and flowing rates: (a) Q_i+Q_o and (b) Q_f.

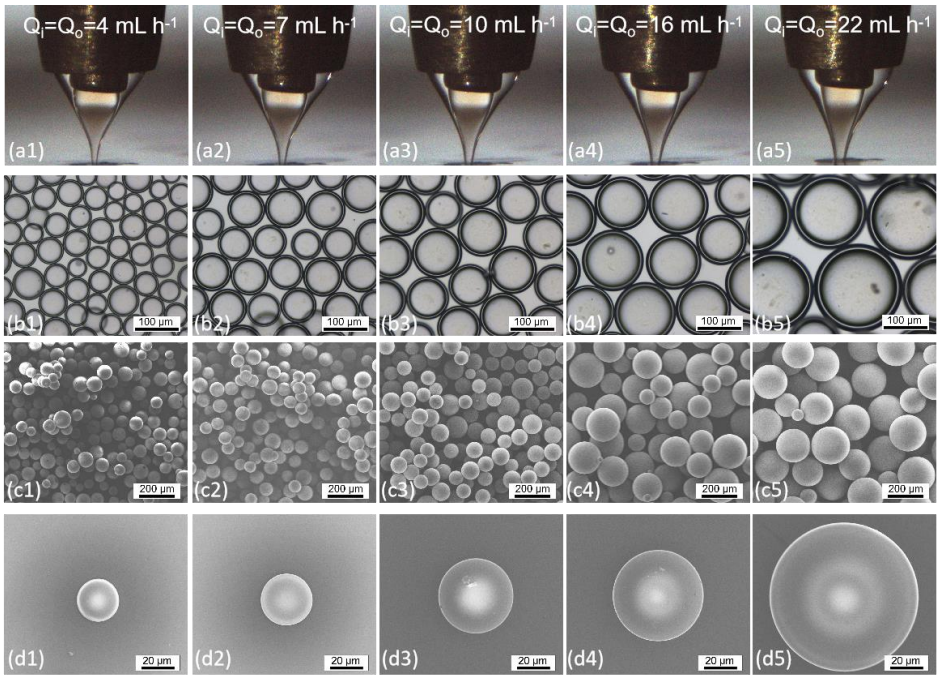

Fig. S10 (a) The steady cone-jet structure and corresponding (b) optical, (c) low- and (d) high-magnification SEM images of the microcapsules. The liquid flow rate of Q_i is the same as Q_o, and the Q_f is fixed at 700 mL h^{-1}.

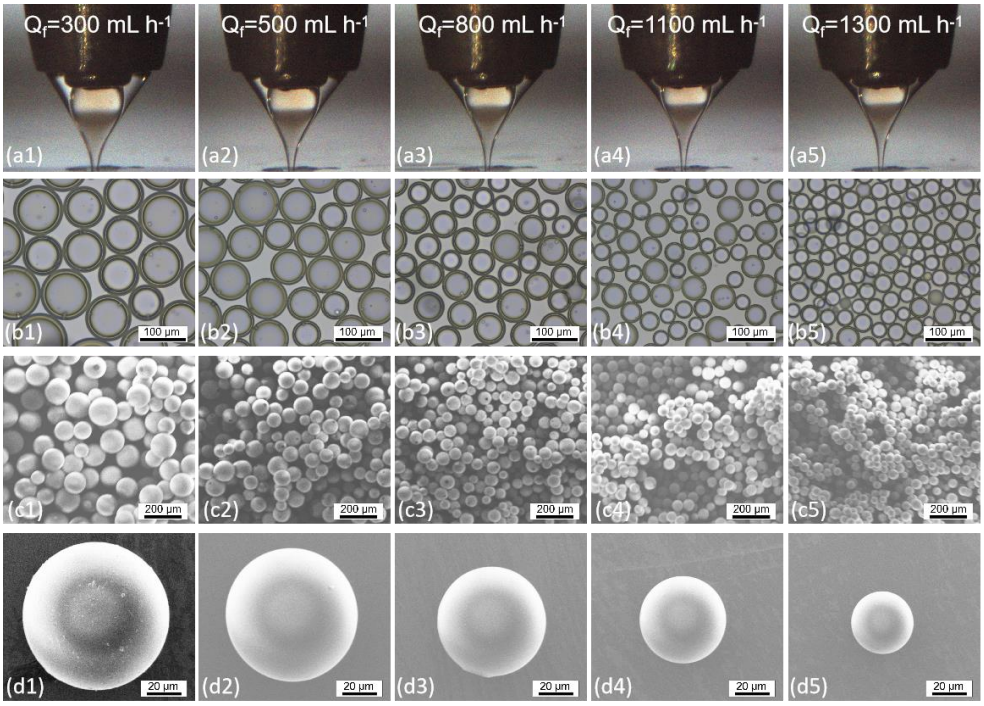

Fig. S11 (a) The steady cone-jet structure and corresponding (b) optical, (c) low- and (d) high-magnification SEM images of the microcapsules. The liquid flow rate of Q_i is 3 mL h^{-1} and Q_o is 4 mL h^{-1}.

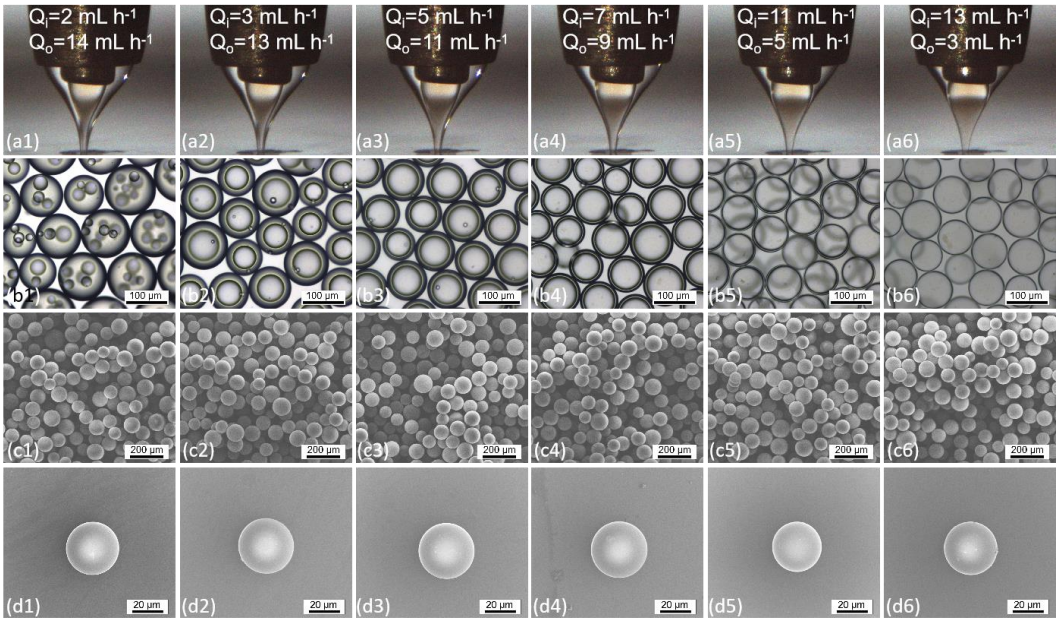

Fig. S12 (a) The stable cone-jet mode changing with φ (φ=Q_i/Q_o), and corresponding (b) optical, (c) low- and (d) high-magnification SEM images of the microcapsules. The sum of the liquid flow rates of the Q_i and Q_o are constant at 16 mL h^{-1}, and the Q_f maintains at 700 mL h^{-1}.

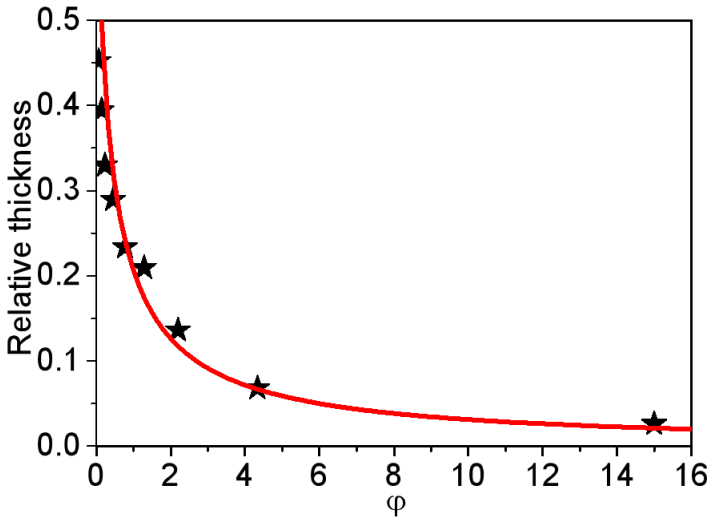

Fig. S13 Relationship of relative thickness *vs* inner and outer phases (φ=Q_i/Q_o).

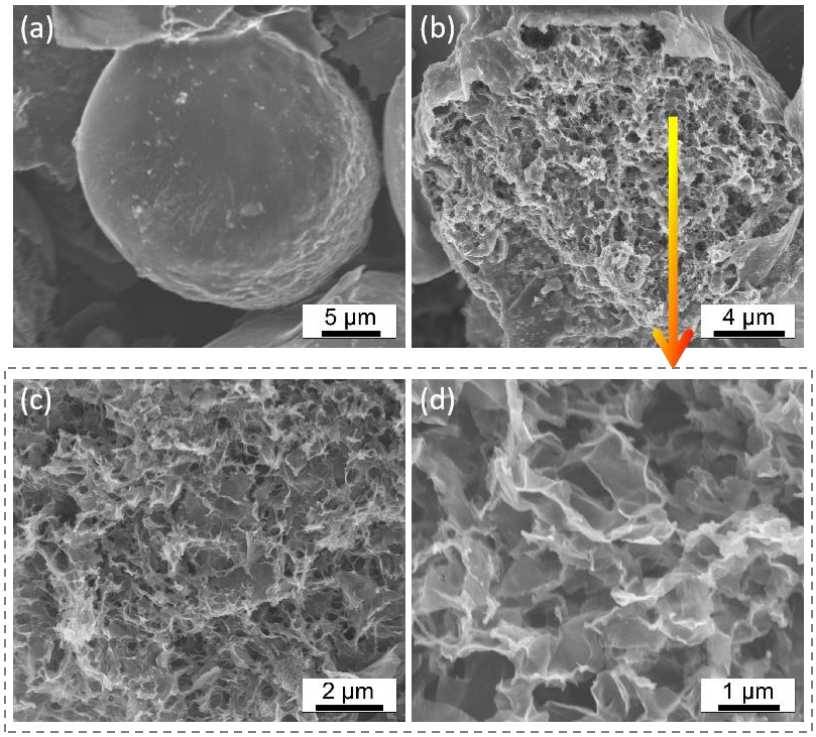

Fig. S14 (a-d) SEM images of the GSMs-H after cycling at 0.2C for 200 cycles.

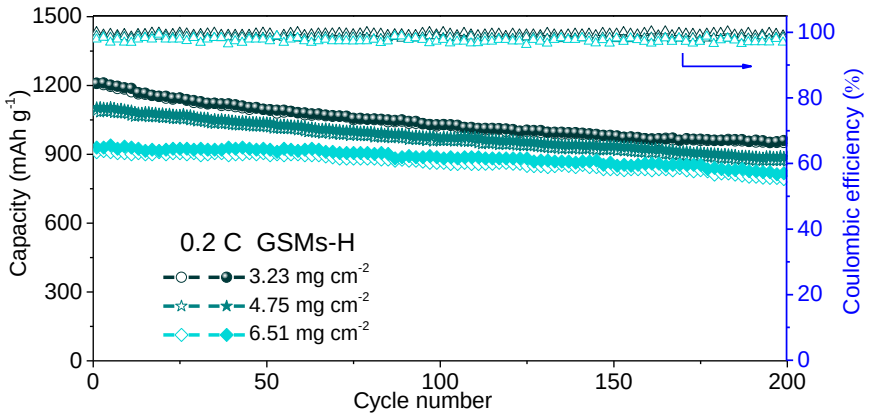

Fig. S15 Cycling capacity of GSMs-H sample with different sulfur loadings.

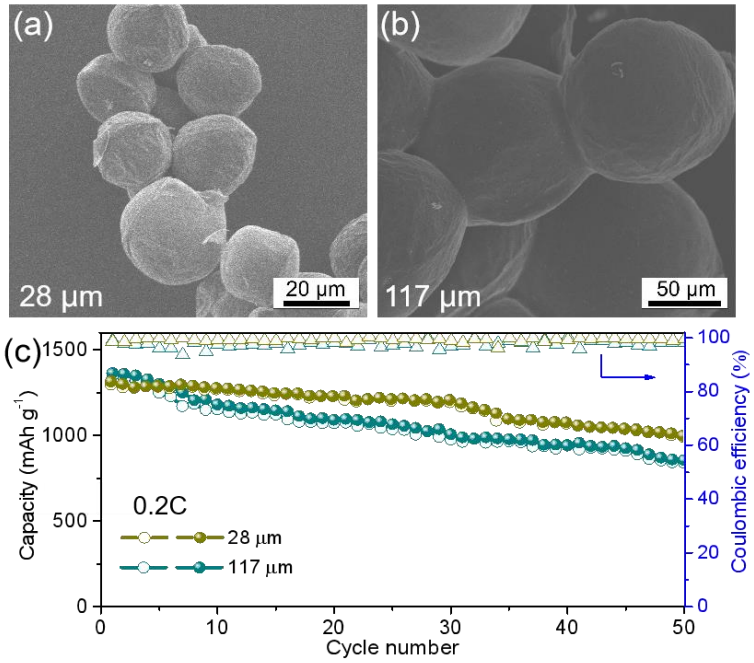

Fig. S16 SEM images of the GSMs-H for the diameters of (a) 28 μm (liquid flow rate: Q_i=2 mL h^{-1}, Q_o =2 mL h^{-1}, Q_f =700 mL h^{-1}) and (b) 117 μm (liquid flow rate: Q_i=3 mL h^{-1}, Q_o =4 mL h^{-1}, Q_f =300 mL h^{-1}). (c) Cycling performance at 0.2C.

Table S1. Comparison on the cycling performance of some GO-based cathodes.

Cathode	Synthetic method	Cycling rate	Cycle number	Capacity (mAh g^{-1})	Ref.
GO paper/S	Modified Hummers' method	100 mA g^{-1}	40	565	1
Mg ZIF-67/ CNT@GO/S	Spray drying	0.1C	50	641	2
$SrTiO_3$@rGO/S	Hydrothermal method	1C	600	820	3
NiS_2/rGO/S	Microwave-assisted method	1C	800	400	4
MnS/(N/S)-rGO/S	Hydrothermal process	0.2C	200	817	5
COF@GO/S	Spray-drying process	1C	500	601	6
Co/NrGO/S	Modified Hummers' method	0.2C	250	905	7
3D N-doped rGO/Co-Ni-S	One-step hydrothermal method	1C	350	700	8

N, S-doped graphene	*In situ* self-assembly	1C	500	622	9
S/Cr-Ni-NDs@G	Hydrothermal reaction	1C	500	682	10
Co@TiO_2/GO/S	Hydrothermal reaction	1C	500	807	11
Co-LDH@rGO/S	Spray-drying process	1C	600	600	12
GO/S-encapsulated microcapsules	Co-flow focusing approach	0.2C	200	1004	This work
		1C	1000	800	

Reference

1 M. Hakimi, Z. Sanaee, S. Ghasemi and S. Mohajerzadeh, *J. Phys. D: Appl. Phys.*, 2022, **55**, 165504.

2 J. Jiang, H. Wang, J. Zhao, J. Li, G. Liu and Y. Zhang, *J. Alloy compd.*, 2022, **899**, 163240.

3 X. He, Z. Lei, H. Liu, S. Wang, T. Qiao and X. Wang, *J. Alloy compd.*, 2022, 898, 162987.

4 Y. Li, J. Chen, Y. Zhang, Z. Yu, T. Zhang, W. Ge and L. Zhang, *J. Alloy compd.*, 2018, **766**, 804-812.

5 Z. Li, R. Xu, S. Deng, X. Su, W. Wu, S. Liu and M. Wu, *Appl. Surf. Sci.*, 2018, **433**, 10-15.

6 Z. Hu, G. Yan, J. Zhao, X. Zhang, Y. Feng, X. Qu, H. Ben, J. Shi, Nanotechnology 2022, 12, 4568.

7 L. Gai, C. Zhao, Y. Zhang, Z. Hu and Q. Shen, *Carbon Energy* 2022, 3, 115.

8 P. Wu, L. Tan, X. Wang, P. Liao, Z. Liu, P. P. Hou, Q. Y. Zhou, X. J. Jin, M. C. Li and X. R. Shao, *Mater. Res. Bull.*, 2022, **145**, 111550.

9 X. Li, Y. Yu, Z. Tang, Y. Yang, Y. Li, J. Cao and L. Chen, *Phys. Chem. Chem Phys.*, 2022, **24**, 2879-2886.

10 J. Zhang, S. Zheng, D. Sun, J. Li and G. Liu, *J. Electroanal. Chem.*, 2021, **902**, 115810.

11 X. Zhang, T. Wan, A. Jia, J. Li, G. Liu, D. Sun and Y. Wang, *Electrochimi. Acta* 2021, **397**, 139264.

12 R. Xiao, W. Qiu, M. Yang, Y. Zhang and X. Wang, *ACS Appl Energ. Mater.*, 2021, 4, 12623-12630.